

Ballistic Quantum Dots with Disorder and Interactions: A numerical study on the Robnik-Berry billiard

Ganpathy Murthy¹, R. Shankar², and Harsh Mathur³

¹*Department of Physics and Astronomy, University of Kentucky, Lexington KY 40506-0055*

²*Department of Physics, Yale University, New Haven CT 06520*

³*Physics Department, Case Western Reserve University, Cleveland, OH 44106-7079*

(Dated: November 16, 2018)

In previous work we have found a regime in ballistic quantum dots where interelectron interactions can be treated asymptotically exactly as the Thouless number g of the dot becomes very large. However, this work depends on some assumptions concerning the renormalization group and various properties of the dot obeying Random Matrix Theory predictions at scales of the order of the Thouless energy. In this work we test the validity of those assumptions by considering a particular ballistic dot, the Robnik-Berry billiard, numerically. We find that almost all of our predictions based on the earlier work are borne out, with the exception of fluctuations of certain matrix elements of interaction operators. We conclude that, at least in the Robnik-Berry billiard, one can trust the results of our previous work at a qualitative and semi-quantitative level.

PACS numbers: 73.50.Jt

I. INTRODUCTION

The quest for a satisfactory theory of quantum dots is driven not only by their obvious importance as mesoscopic devices revealed by a series of groundbreaking experiments[1], but also by their challenge as a unique confluence of disorder, interactions and finite-size effects[2]. For weak interactions, the Universal Hamiltonian[3, 4] (UH) provides a satisfactory description. For ballistic/chaotic quantum dots, we have espoused[5, 6, 7] an approach based on the fermionic Renormalization Group[8] (RG), $1/N$ expansions and the fact that energy eigenstates around the Fermi energy in disordered systems ought to be described by Random Matrix Theory (RMT)[9, 10]. Our approach not only explains the UH as a fixed point of the RG but also describes the physics outside its basin of attraction. It predicts a phase transition at strong coupling and allows a fairly detailed study[7] of the new phase and the quantum critical region[11] separating it from that governed by the UH.

Our results, however, were predicated on a variety of RMT and RG assumptions. To test our assumptions and the conclusions deduced from them, we performed a detailed numerical study on a ballistic but chaotic billiard (the Robnik-Berry billiard[12]) and we report our findings here. Our expectations are borne out, with one notable exception.

We recall our strategy and assumptions briefly so that the reader may see in advance what sort of ideas are put to test in our study. In the primordial problem of interest to us one has electrons confined to a ballistic dot of size L , with no impurities inside, and edges so irregular that classical motion is chaotic. The electrons experience the Coulomb interaction. In momentum space, all momenta within the bandwidth (of order k_F , the Fermi momentum) exist. The semiclassical ergodicization time for an electron within the dot is a few bounces, or $\tau_{erg} \simeq L/v_F$.

By the uncertainty principle this leads to an important energy scale, the Thouless energy $E_T \simeq \hbar v_F/L$ which has a dual significance. First, it controls the dimensionless conductance of a dot strongly coupled to leads, as follows. Since the transport through the dot takes place in a time such that energy is uncertain by an amount E_T , all single particle states that fit into this band will each contribute a unit of dimensionless conductance. If the average single-particle level spacing is δ , then the dimensionless conductance is $g = E_T/\delta$. Second, in the other limit of dots very weakly coupled to leads (which we focus on in this work), the Thouless band of width E_T centered on E_F , marks the scale deep within which RMT should apply to the energies and eigenfunctions[9]. In this context g is better denoted the Thouless number.

Since we are only interested in a narrow band of energies of width $E_T \ll E_F$, the first step in the program[5] is to use the RG for fermions[8] to get an effective low energy theory by eliminating all momentum states outside E_T . Should we worry that we are not eliminating exact single particle eigenstates (labelled here by α)? No, because the disorder due to the boundaries will mix momentum states at roughly the same energy, and it does not matter whether we eliminate momentum states within any annulus of energy thickness E_T or the single particle states they evolve into. Indeed, even the mixing within E_T is due to the fact that momentum itself not well defined in a finite dot, a point we will elaborate on shortly. However, once we come down to within E_T of E_F , we cannot eliminate the remaining states in one shot since it is the flow of couplings *within* this band that is all important in the RG.

Now it is known[8] that the clean system RG (justified above) leads to Landau's Fermi liquid interaction[13]

$$V = \sum_{\mathbf{k}\mathbf{k}'} F(\theta_{\mathbf{k}} - \theta_{\mathbf{k}'}) \delta n(\mathbf{k}) \delta n(\mathbf{k}') \quad (1)$$

at an energy scale E_L which is small compared to E_F .

But since E_L is a bulk scale it can always be made larger than E_T which vanishes as $L \rightarrow \infty$. Thus Murthy and Mathur[5] perform their RG on the hamiltonian (focussing on the spinless case for simplicity)

$$H = \sum_{\alpha} c_{\alpha}^{\dagger} c_{\alpha} \varepsilon_{\alpha} + \sum_{\alpha\beta\gamma\delta} V_{\alpha\beta\gamma\delta} c_{\alpha}^{\dagger} c_{\beta}^{\dagger} c_{\gamma} c_{\delta} \quad (2)$$

where

$$V_{\alpha\beta\gamma\delta} = \frac{1}{4} \sum_{\mathbf{k}\mathbf{k}'} F(\theta_{\mathbf{k}} - \theta_{\mathbf{k}'}) (\phi_{\alpha}^*(\mathbf{k}) \phi_{\beta}^*(\mathbf{k}') - \phi_{\beta}^*(\mathbf{k}) \phi_{\alpha}^*(\mathbf{k}')) \times (\phi_{\gamma}(\mathbf{k}') \phi_{\delta}(\mathbf{k}) - \phi_{\delta}(\mathbf{k}') \phi_{\gamma}(\mathbf{k})) \quad (3)$$

is simply the Landau interaction written in the basis of exact eigenstates, a statement that needs some elaboration. In usual RMT treatments, $\phi_{\alpha}(\mathbf{k})$ is the exact eigenstate α written in the infinite dimensional basis of all momentum states. In our version which uses the RG to reduce the Hilbert space, the states labeled by \mathbf{k} are approximate momentum states with an uncertainty $\delta k \simeq 1/L$ in both directions. The number of such wave packets that fit into an annulus of radius k_F and thickness E_T/v_F is $\mathcal{O}(k_F L) = g$. We call them the Wheel-of-Fortune (WOF) states, see Figure (1). One way to construct such packets is to pick g plane waves of equally spaced momenta on the Fermi circle and to chop them off at the edges of the dot to respect the boundary conditions. This is what we mean by \mathbf{k} in $\phi_{\alpha}(\mathbf{k}) = \langle \mathbf{k} | \alpha \rangle$.

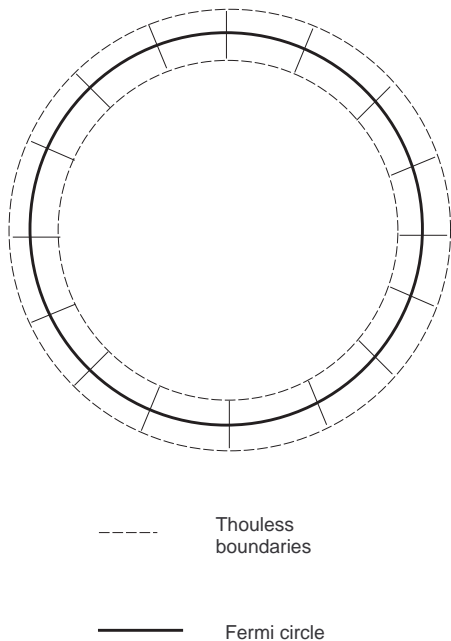


FIG. 1: The g wheel-of-fortune states in the Thouless band. They are packets in \mathbf{k} space with average momenta equally spaced on the Fermi circle.

We are now ready to state our two assumptions.

Assumption 1: *We assume that the g approximate momentum states generated as above form a complete basis for the g exact eigenstates in the Thouless shell.*

Assumption II: The energy eigenvalues ε_{α} obey RMT statistics as do the wavefunctions. For example we assume that the ensemble averages (denoted by $\langle \rangle$) obey

$$\langle \phi_{\mu}^*(\mathbf{k}_1) \phi_{\mu}(\mathbf{k}_2) \phi_{\nu}^*(\mathbf{k}_3) \phi_{\nu}(\mathbf{k}_4) \rangle = \frac{\delta_{12} \delta_{34}}{g^2} + O(1/g^3) \quad (4)$$

To some, Assumption I seems remarkable – How can we furnish *in advance, independent of the dot shape* a basis of g states for expanding the g exact eigenstates within E_T ? After all, these eigenstates are supposed to resemble those of a random matrix. The point is that no matter how chaotic the dot, it can only mix states at the same energy. While this sounds like Berry’s ansatz[14] it is somewhat different in both scope and content: Berry’s ansatz states that every exact eigenstate α can be expanded in terms of an *infinite number* of \mathbf{k} states (with the same energy $\varepsilon_{\alpha} = \mathbf{k}^2/2m$) in the bulk, while we claim that only g of WOF states are needed. Secondly, we claim that the *same* g WOF states can be used to describe all the states within the Thouless band.

In this work we will show that these states are nearly orthonormal and that the exact state right in the middle of the band has 99.9% overlap with the WOF states. The success of this extension of Berry’s conjecture to a finite dot exceeds our expectations in this regard. However, we find that the g WOF states become less effective at describing states as we move away from E_F : the overlap drops to 50% at $E_{\alpha} = E_F \pm E_T/2$. This prepares us for the possibility that nonuniversal quantities may be quantitatively inaccurate in our approach.

As for Assumption II, we have verified RMT behavior for the eigenvalues (as have others before us[15, 16]) but not the eigenfunctions. What we did instead was to see what extent the solution of a specific dot resembled the picture we drew based on these two assumptions. We begin by describing how one starts from Eqn. (3), which describes the effective hamiltonian, and use our two assumptions with large- N ideas to make our predictions[6, 7]. These predictions are asymptotically exact as $g \rightarrow \infty$.

First one expands the Landau function as

$$F(\theta) = \sum_m u_m e^{im\theta}. \quad (5)$$

Barring accidents, the phase transition occurs in one channel with some m (recall superconductivity). This allows us to focus on a single $u_m \neq 0$, ignoring all others. Then we carry out a Hubbard-Stratovich transformation on the interaction using a collective field σ . We then formally integrate out the fermions and get an effective action $S(\sigma)$ for σ . In this process we make use of assumption II. The action in terms of σ is obtained by summing one loop Feynman diagrams with varying numbers of external σ ’s connected to a single fermion line running around the loop. Each diagram is a sum over fermion energy denominators multiplying products

of a string of $\phi_\alpha(\mathbf{k})$'s. We are able to show that these products may be replaced by their ensemble averages in the large g limit. In other words the sum over so many terms in each diagrams leads to self-averaging. For the averages we use relations like Eqn. (4). When this is done, the effective action can be cast into a form which has a g^2 in front of it[6, 7], so that the saddle point gives exact answers as $g \rightarrow \infty$.

At this point let us collect all the results and predictions of the RMT + large- N theory[7] with a view to comparing them with similar results without using Assumptions I and II on the Robnik-Berry billiard.

- In the large- g limit there is a sharp transition to a phase in which σ acquires a vacuum expectation value. The critical value of u_m in our approximation turns out to be $-1/\log 2$ in the spinless case and $-1/2 \log 2$ in the spinful case. The true critical value is most likely to be the bulk value -2 (spinless) or -1 (spinful), as has been found in an explicitly solvable model by Adam, Brouwer, and Sharma recently[18]. This is an example of the nonuniversal quantity alluded to earlier, that we cannot predict exactly in our approach even as $g \rightarrow \infty$.
- For finite g , instead of a sharp phase transition, there is a crossover from the weak-coupling regime through a quantum critical regime to a strong-coupling regime. Due to the explicit symmetry-breaking at order $1/g$, there is always some nonzero order parameter, which increases to a number of order g (in the normalization we use here, which is different from that of ref.[7]) in the strong-coupling regime.
- For symmetry-breaking in odd angular momentum channels there are two exactly degenerate minima for every sample arising from time-reversal invariance.
- The ground state energy at the minimum in the strong-coupling regime is lower than that in the weak-coupling regime by a number of order $g^2\delta$.
- The effective potential landscape in the strong-coupling regime is in the approximate shape of a Mexican Hat, with the ripples at the bottom of the hat being of order $g\delta$.
- In the quantum-critical and strong-coupling regimes, even low-energy quasiparticles acquire large widths given on average by

$$\Gamma(\varepsilon) \approx \frac{\delta}{\pi} \log(\varepsilon/\delta) \quad (6)$$

We found that most of these predictions are verified by our numerical results on the Robnik-Berry billiard, except that the ripples at the bottom of the Mexican Hat turn out to be much larger than expected for the $m = 2$ Landau interaction channel.

II. THE ROBNIK-BERRY BILLIARD

In this section we will describe how the dot is chosen and how the single particle energy levels ε_α and eigenfunctions $\phi_\alpha(\mathbf{r})$ are determined. We use a trick invented by Robnik and Berry[12] and elaborated upon by Stone and Bruus[15]. Consider a unit circle $|z| = 1$ in the complex plane of $z = x + iy$. The analytic function

$$w(z) = \frac{z + bz^2 + cz^3 e^{i\chi}}{\sqrt{1 + 2b^2 + 3c^2}} \quad (7)$$

defines a map under which the unit circle in z gets mapped into a new shape in w , which will be our dot. The shape of the dot can be varied by varying the parameters b , c , and χ . The denominator ensures that the billiard has the same area (π) as the unit disc. The wavefunction $\phi_\alpha(w, \bar{w}) = \phi_\alpha(u, v)$ is required to vanish at the boundary and obey

$$\begin{aligned} & - \left(\frac{\partial^2}{\partial u^2} + \frac{\partial^2}{\partial v^2} \right) \phi_\alpha(u, v) \\ & = -4 \frac{\partial}{\partial w} \frac{\partial}{\partial \bar{w}} \phi_\alpha(w, \bar{w}) = \varepsilon_\alpha \phi_\alpha(w, \bar{w}). \end{aligned} \quad (8)$$

(We have chosen $\hbar = 2m = 1$). If we now go the z plane where the wavefunction is $\phi_\alpha(w(z), \bar{w}(\bar{z}))$, the Schrödinger equation and boundary condition are

$$-4 \frac{\partial}{\partial z} \frac{\partial}{\partial \bar{z}} \phi_\alpha(z, \bar{z}) = \varepsilon_\alpha |w'(z)|^2 \phi_\alpha(z, \bar{z}) \quad \phi_\alpha(|z| = 1) = 0 \quad (9)$$

where $w'(z) = dw/dz$. This differential equation in the continuum is next converted to a discrete matrix equation by writing

$$\phi_\alpha(z, \bar{z}) \equiv \phi_\alpha(r, \theta) = \sum_j \frac{1}{\gamma_j} C_j^\alpha \psi_j(r, \theta) \quad (10)$$

where $\psi_j(r, \theta)$ is the solution to the free Schrödinger equation in the unit disk vanishing on the boundary:

$$-\nabla^2 \psi_j(r, \theta) = \gamma_j^2 \psi_j(r, \theta). \quad (11)$$

(That is, these are Bessel functions in r times angular momentum eigenfunctions in θ .) Feeding this expansion into Eqn. (9) one obtains the matrix equation

$$\sum_j M_{ij} C_j^\alpha = \frac{1}{\varepsilon_\alpha} C_i^\alpha \quad (12)$$

where

$$M_{ij} = \frac{1}{\gamma_i} \langle i | |w'|^2 | j \rangle \frac{1}{\gamma_j}. \quad (13)$$

(Without the $1/\gamma_j$ in the expansion Eqn. (10), M would not have been Hermitian.)

In practice one truncates M to a finite size (we used 585 states) and expects the lower energy levels and wavefunctions to be unaffected.

The parameters b, c, χ are chosen to lie in the range where classical behavior is chaotic, and where quantum chaos as reflected in the eigenvalue distribution has been established[15]. A value we used repeatedly was $b = c = .2, \chi = .85$. A nonzero χ ensures that the billiard has no reflection symmetry. This shape is often called the Africa Billiard based on its resemblance to that continent, as seen in Fig 2 for our chosen values of parameters.

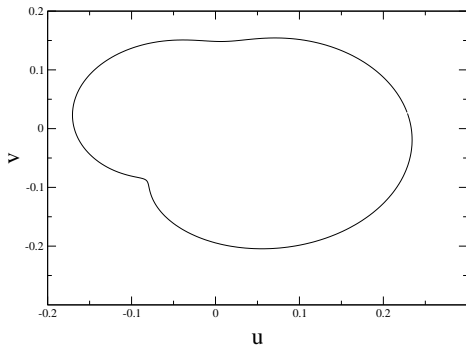


FIG. 2: The shape of the Robnik-Berry billiard for $b = c = 0.2$, and $\chi = 0.85$.

We shall refer to these eigenfunctions and eigenvalues as exact even though they come from solving a truncated problem because we can easily increase the accuracy by increasing the size of the truncated Hilbert space.

A. Testing Assumptions I and II

Our ability to solve the Schrödinger equation (to high accuracy) implies in principle that we can test our two assumptions.

In the next subsection we will test Assumption I, i.e., see in detail how well the WOF states serve a basis within the Thouless band.

As for Assumption II, we and our predecessors [15, 16] have shown that the eigenvalues and single eigenfunctions obey the distribution expected by RMT for a GOE. (The ensemble is generated by varying the parameters in $w(z)$.)

Similar information about wavefunction correlations is not known in the ballistic problem (despite some recent progress using supersymmetry methods[17]). We did not try to do this here since our computing capabilities did not allow us to generate an ensemble.

Instead we computed the fate of the interacting system without recourse to Assumptions I and II and compare to our predictions based on these assumptions.

B. Completeness of the WOF basis

Let E_F be the Fermi energy. Then $g \simeq \sqrt{4\pi N} \simeq \sqrt{\pi E_F}$, which we arrive at as follows. The Fermi circle has a circumference $2\pi K_F$ and into this will fit

$g = 2\pi K_F / (2\pi/L)$ WOF states each of width $2\pi/L$ in the tangential direction. Finally $E_F = K_F^2/2m = K_F^2$, $N = k_F^2 L^2 / 4\pi$ and $L = \sqrt{\text{Area}} = \sqrt{\pi}$.

As a test case when we picked the Fermi energy to be the 100-th level, we found $g = 37$. How well is this state $|F\rangle$ at E_F spanned by the g WOF states at the Fermi energy?

First we first take g equally spaced points \mathbf{k}_n on the Fermi circle and form the WOF states

$$\psi_{WOF-n}(\mathbf{r}) = \frac{1}{\sqrt{\pi}} e^{i\mathbf{k}\cdot\mathbf{r}} \Theta(\text{dot}) \quad (14)$$

where $\Theta(\text{dot})$ is unity inside the dot and zero outside. These states are very close to being orthonormal. For example the overlaps of $n = 1$ state (with \mathbf{k} along the y -axis) with the others as we go around the circle is shown in Fig. (3).

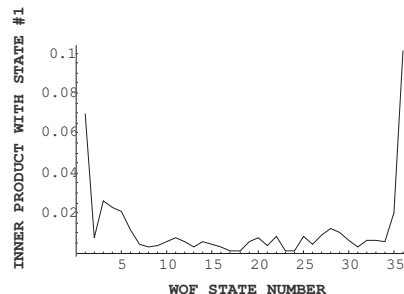


FIG. 3: The absolute value of $\langle n|1\rangle$, the inner product of WOF state number 1 with the other $g - 1 = 36$ states.

Next we ask how much of the state $|F\rangle$ at the Fermi energy is contained in the WOF states. We find $\sum_{n=1}^g |\langle n - WOF|F\rangle|^2 = .9993$. This is a rather remarkable result. It says that $|F\rangle$, which is a vector with 580 components (which was the size of our truncated problem) can be expanded almost completely in terms of $g = 37$ WOF states which are given in advance. In other words as one changes the shape of the dot and works at fixed Fermi energy, the state $|F\rangle$ changes in a random way, but that randomness is only in which particular combination of WOF states describes it, not in the completeness of the WOF basis.

While this is very satisfactory we need more to implement our scheme: we need to be expand all g states in the WOF basis. Here we find that as we move off the center of the Thouless band, the fractional norm captured by the WOF basis drops. In a typical case, with $g = 37$, there are roughly 12 states (one third of g) where the

number lies above 95%. At band edge this drops to 50%, as shown in Fig (4). Thus there is inevitably some error in transcribing the Landau interaction written in terms of the WOF states labelled by \mathbf{k} into the basis of g exact eigenstates labelled by α . This just means that the location of the critical point will not be correctly predicted by our RMT based analysis, as pointed out recently by Adam, Brouwer, and Sharma[18].

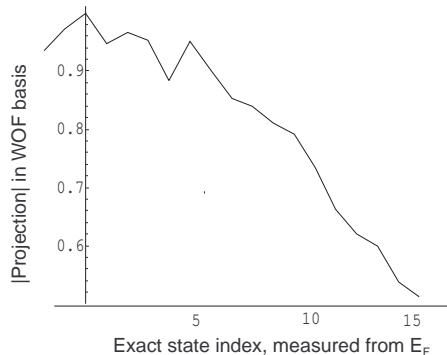


FIG. 4: The norm of the projection of the n^{th} exact eigenstate from E_F on to the subspace spanned by the WOF states. It can be seen that more and more of the exact eigenstate lies outside this subspace as one moves away from E_F .

This concludes our (partial) test of Assumptions I and II. We turn to a comparison of our results based on these assumptions with a direct solution of the problem with no recourse to the assumptions.

C. Hartree-Fock solution of interacting problem

How can the knowledge of the "exact" eigenfunctions and eigenvalues in the billiard help in the solution of the problem with interactions? The tactic will be illustrated in schematic form first. Suppose we have a four-Fermi interaction added to a free hamiltonian which in first-quantization is given by some differential operator H_0 . Then the path integral becomes

$$Z = \int d\psi d\bar{\psi} e^S \quad (15)$$

where

$$S = \int d\tau \left[\bar{\psi} (i\partial_\tau - H_0) \psi + \frac{u}{2} (\bar{\psi}\psi)^2 \right]. \quad (16)$$

Using a Hubbard-Stratanovich transformation we can write

$$Z = \int d\psi d\bar{\psi} d\sigma e^S \quad (17)$$

where

$$S = \int d\tau \left[\bar{\psi} [i\partial_\tau - H_0 - \sigma] \psi - \frac{\sigma^2}{2u} \right]. \quad (18)$$

If the fermions are integrated out we will get an effective action $S_{eff}(\sigma)$. To find the minimum we need just the action for static σ . In this case it is clear that

$$\int d\psi d\bar{\psi} \exp \left[\int d\tau \bar{\psi} [i\partial_\tau - H_0 + \sigma] \psi \right] = e^{-E_0(\sigma)T} \quad (19)$$

where $T \rightarrow \infty$ is the length of the imaginary time τ - axis and $E_0(\sigma)$ is the ground state energy of $\psi^\dagger (H_0 + \sigma) \psi$. To find $E_0(\sigma)$ one simply solves for the single particle levels of $(H_0 + \sigma)$ and fills up the ones with negative energy. The effective action for static configurations, which is also the effective potential, is

$$V_{eff} = E_0(\sigma) + \frac{\sigma^2}{2u}. \quad (20)$$

At this point we have a mean-field theory. We still need to justify its use by showing that fluctuations of the collective field σ around its minimum are small. In our previous work, based on Assumptions I and II we showed that the fluctuations were indeed small in the limit of large g , since the g^2 in front of the actions limits fluctuations. In the billiard we will justify the mean field similarly, based on the depth and curvature of the minimum.

When the Landau interaction is factorized, the hamiltonian whose ground state gives us $E_0(\sigma)$ is

$$\sum_{\alpha\beta} \psi_\alpha^\dagger (\delta_{\alpha\beta} \varepsilon_\beta + \sigma \cdot \mathbf{M}_{\alpha\beta}) \psi_\beta \quad (21)$$

where, for the case $m = 1$, for example,

$$\mathbf{M}_{\alpha\beta} = \sum_{\mathbf{k}} \phi_\alpha^*(\mathbf{k}) \phi_\beta(\mathbf{k}) \frac{\mathbf{k}}{k} \quad (22)$$

and $\alpha, \beta, \mathbf{k}$ are not restricted to the Thouless band. This is because we want to solve the problem without any of the assumptions that led to the effective low energy theory within the Thouless band. Note that σ has two components, because the Landau interaction associated with u_m has two parts:

$$V_L = \frac{u_m}{2} \sum_{\mathbf{k}\mathbf{k}'} \delta n_{\mathbf{k}} \delta n_{\mathbf{k}'} (\cos m\theta_{\mathbf{k}} \cos m\theta_{\mathbf{k}'} + \sin m\theta_{\mathbf{k}} \sin m\theta_{\mathbf{k}'}). \quad (23)$$

Once S_{eff} is known (on a grid of points in the σ plane) one can ask if and when the minimum moves off the origin.

So far our considerations have been fairly generic, and the Landau interaction has been written in momentum space. However, in testing our approach in the billiard, we will find it more convenient to represent the Landau interaction in real space, since the eigenfunctions are

known as linear combinations of Bessel functions whose integrals are best carried out in real space. We have carried out calculations for two Landau parameters corresponding to $m = 1$ and $m = 2$. The $m = 1$ Landau interaction is chosen to be (in second-quantized notation)

$$\frac{1}{2} \int d^2r \Psi^\dagger(\vec{r}) \frac{1}{(2mH_0)^{1/4}} (-i\vec{\nabla}) \frac{1}{(2mH_0)^{1/4}} \Psi(\vec{r}) \cdot \\ \times \int d^2r' \Psi^\dagger(\vec{r}') \frac{1}{(2mH_0)^{1/4}} (-i\vec{\nabla}') \frac{1}{(2mH_0)^{1/4}} \Psi(\vec{r}') \quad (24)$$

The factors of $\frac{1}{(2mH_0)^{1/4}}$ on each side of the ∇ have the effect of $1/|\mathbf{k}|$ in momentum space. Since momentum does not commute with the free Hamiltonian H_0 , the factors have to be placed symmetrically. Note that this corresponds only to the $\vec{q} = 0$ part of the Landau interaction. In reality, all values of \vec{q} up to the scale E_L/v_F exist in the Hamiltonian. Depending on the shape of the dot a particular combination of them may break symmetry to give the best energy. Still, we expect that since at large g we are close to the zero-dimensional limit, the best combination will consist largely of very small \vec{q} parts of the Landau interaction. In any case, the energy of the true symmetry-broken state can only be lower than what we calculate, so what we have here is a conservative estimate of symmetry-breaking. Similarly the $m = 2$ interaction (also at $\vec{q} = 0$) is

$$\frac{1}{2} \int d^2r \Psi^\dagger(\vec{r}) \frac{1}{(2mH_0)^{1/2}} (\nabla_x^2 - \nabla_y^2) \frac{1}{(2mH_0)^{1/2}} \Psi(\vec{r}) \cdot \\ \times \int d^2r' \Psi^\dagger(\vec{r}') \frac{1}{(2mH_0)^{1/2}} ((\nabla'_x)^2 - (\nabla'_y)^2) \frac{1}{(2mH_0)^{1/2}} \Psi(\vec{r}') \\ + \frac{1}{2} \int d^2r \Psi^\dagger(\vec{r}) \frac{1}{(2mH_0)^{1/2}} 2\nabla_x \nabla_y \frac{1}{(2mH_0)^{1/2}} \Psi(\vec{r}) \\ \times \int d^2r' \Psi^\dagger(\vec{r}') \frac{1}{(2mH_0)^{1/2}} 2(\nabla'_x)(\nabla'_y) \frac{1}{(2mH_0)^{1/2}} \Psi(\vec{r}') \quad (25)$$

The integrals are over (w, \bar{w}) , but can be converted to integrals over the disk by using the conformal mapping of Eq. (7). Of course, the derivative operators must also be transformed in the process. In order to find the matrix elements of $\mathbf{M}_{\alpha\beta}$ we had to take the matrix elements of the above operators in the basis of exact billiard states. We carried out the angular part of the integrals analytically, but had to turn to numerical integration to evaluate the radial integrals. This is a computationally intensive calculation, but once the matrix \mathbf{M} has been constructed, one simply diagonalizes the Hamiltonian of Eq. (21) for a mesh of σ in the plane, adds up the energies of the lowest N particles to obtain the fermionic ground state energy, and obtains the effective potential landscape from Eq. (20) for various values of the coupling strength u . After this, it is a simple matter to identify the global minimum, which gives us the lowering of ground state energy and the value of the order parameter as a function of u .

Let us proceed to the results, displayed in pictorial form. In Fig. 5 we show the absolute value of the order parameter, normalized by the nominal value of $g = \sqrt{4\pi N}$, for three values of the number of particles N . The bulk transition happens at $u_{bulk}^* = 2$. As can be seen, there is a nonzero order parameter for any nonzero

u , and it grows smoothly and continuously as u increases. Nothing discontinuous happens at $u = 2$ or even beyond, indicating that the instability does not suddenly become first-order at the bulk value of u^* . Of course, in these finite systems, the Thouless and bulk scales are related by a factor $g/4\pi$, which is not that large (4.4 for the largest system we considered, with $N = 245$). So somewhere between $u = 2.25$ and $u = 2.5$ the instability seems to reach the bulk scale. However, note that the size of systems we have considered correspond quite closely to actual ballistic samples[1], which typically have a few hundred electrons. Further, the three curves seem to track each other fairly closely, indicating that the expectation value of $|\sigma|$ indeed scales with g , as predicted by our earlier work based on RMT assumptions.

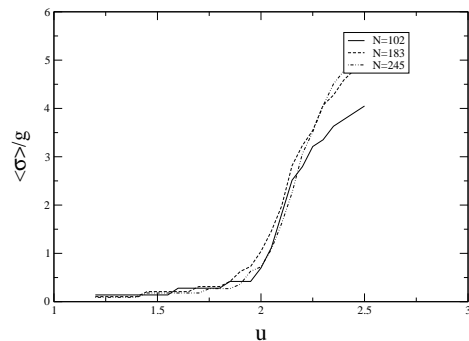


FIG. 5: The absolute value of the order parameter normalized by g as a function of coupling strength u for three values of the number of particles N . The fact that the curves track each other closely indicates that the order parameter does indeed scale like g . Furthermore, nothing discontinuous happens at the bulk critical coupling strength $u_{bulk}^* = 2$.

In Fig. 6 we show the corresponding reduction in ground state energy normalized by g^2 . Once again, the curves track each other fairly closely, indicating that the energy reduction due to interactions is indeed of order g^2 , as predicted by our earlier work.

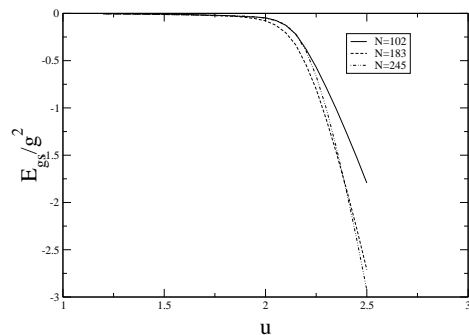


FIG. 6: Reduction in ground state energy normalized by g^2 for three values of the number of particles N .

In Fig. 7 we show the effective potential landscape for $m = 2$, with $N = 245$, at a value of $u = 2.15$, at which the minimum is well-developed, but the order parameter

is still within the nominal Thouless scale and has not reached the bulk scale. The RMT analysis predicted a Mexican Hat landscape with “small” ripples (down by $1/g$) in the circle of minima of the Mexican Hat. The landscape we see bears no resemblance to this. Instead, it appears to be an isolated minimum at a nonzero σ . Upon close inspection it can be seen that the minimum is shallower in the transverse direction than in the radial direction, but this is the only indication we could find of a (perhaps) incipient Mexican Hat structure.

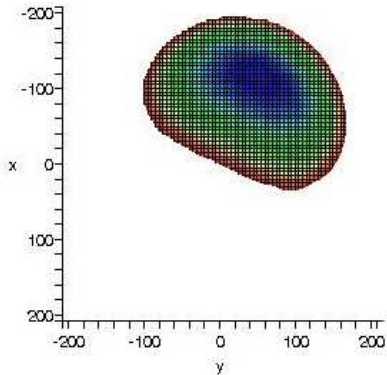


FIG. 7: Effective potential landscape for symmetry-breaking in the $m = 2$ channel. Instead of a Mexican Hat minimum structure with small ripples we see an isolated minimum. The minimum does seem shallower in the transverse direction.

Fig. 8 shows a similar effective potential landscape for symmetry breaking in the $m = 1$, channel, where the two exactly degenerate minima expected from time-reversal invariance considerations can be seen. The landscape also appears more Mexican-Hat-like than in the $m = 2$ case.

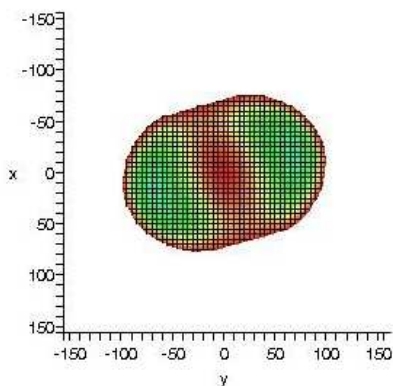


FIG. 8: Effective potential landscape for symmetry-breaking in the $m = 1$ channel for $N = 200$ and $u = 2.15$. The two exactly degenerate minima required by time-reversal invariance can be seen, as can a Mexican-Hat-like structure.

To trace the origin of this difference in behavior, we investigated the average absolute value $\langle |M_{\alpha\beta}^i| \rangle$ and the rms deviation of the matrix elements from the mean absolute value, $\sqrt{\langle |M_{\alpha\beta}^i|^2 \rangle - \langle |M_{\alpha\beta}^i| \rangle^2}$ for the two cases $m = 1, 2$. The results for the $i = 1$ (corresponding to ∇_x for $m = 1$ and $\nabla_x^2 - \nabla_y^2$ for $m = 2$) shown in Fig. 9 are an energy average for a particular billiard, with the parameters $b = c = 0.20, \delta = 0.85$. (We have confirmed similar behavior of the matrix elements for other parameter values as well.) Fig. 9 shows these quantities as a function of the energy difference between the two states α and β . There are two features that are particularly noteworthy.

- There is a “hole” in the $m = 1$ matrix element near zero energy difference.
- The rms deviation of the $m = 2$ matrix elements from their mean absolute value is huge. As a rough estimate, if the matrix elements were Gaussian distributed complex numbers, the rms deviation should be roughly half the mean modulus.

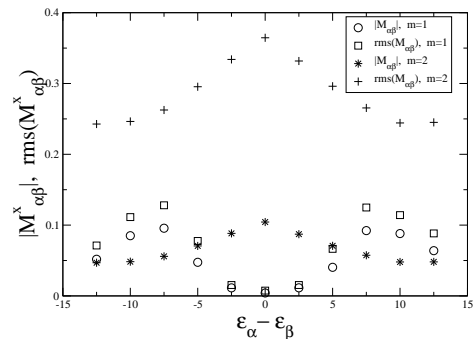


FIG. 9: A plot of the absolute value and the rms deviation of the matrix elements $M_{\alpha\beta}^x$ from their mean absolute value as a function of $\varepsilon_\alpha - \varepsilon_\beta$ for the two cases $m = 1, 2$.

However, the $i = 2$ component (corresponding to ∇_y for $m = 1$ and $2\nabla_x\nabla_y$ for $m = 2$) shows very different behavior in Fig. 10. While the $m = 1$ case looks similar to the $i = 1$ component, the fluctuations of the $m = 2$ $i = 2$ component are strongly suppressed by almost an order of magnitude below the mean.

Consider first the “hole” at E_F for $m = 1$. By symmetry considerations alone one can understand that the diagonal matrix element $M_{\alpha\alpha}$ for $m = 1$ has to be zero sample by sample in the absence of an external magnetic field. Focusing on the x component of the order parameter

$$M_{\alpha\alpha}^x = \sum_{\mathbf{k}} \cos(\theta_{\mathbf{k}}) \phi_{\alpha}^*(\mathbf{k}) \phi_{\alpha}(\mathbf{k}) \quad (26)$$

By time-reversal invariance $\phi_{\alpha}^*(\mathbf{k}) = \phi_{\alpha}(-\mathbf{k})$. Noting that $\theta_{-\mathbf{k}} = \theta_{\mathbf{k}} + \pi$, and that the cos term changes sign, one concludes that $M_{\alpha\alpha}^x = -M_{\alpha\alpha}^x = 0$. The reason the “hole”

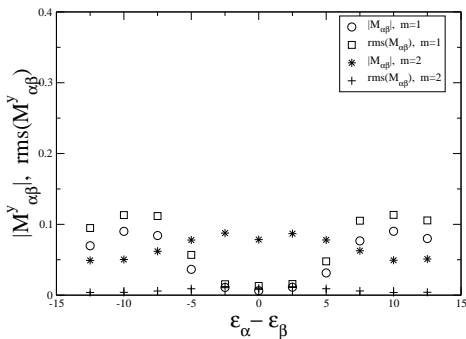


FIG. 10: A plot of the absolute value and the rms deviation of the matrix elements $M_{\alpha\beta}^y$ from their mean absolute value as a function of $\epsilon_\alpha - \epsilon_\beta$ for the two cases $m = 1, 2$.

persists for finite energy differences for the operator $\vec{p} = -i\vec{\nabla}$ can be explained by noting that[19] for a billiard

$$\begin{aligned} \vec{p} &= im[\vec{r}, H] \\ \Rightarrow (-i\vec{\nabla})_{\alpha\beta} &= -im(\vec{r})_{\alpha\beta}(\epsilon_\alpha - \epsilon_\beta) \end{aligned} \quad (27)$$

which means that the matrix element must vanish at least linearly with the energy difference. In fact, such “banded” matrix elements have been found for many operators in ballistic dots[20].

Consider next the fact that the distribution of the matrix elements of $M_{\alpha\beta}^x$ for the $m = 2$ case is much broader than for the $m = 1$ case, while the $M_{\alpha\beta}^y$ matrix elements have a very narrow distribution. The RMT answer would have the rms deviation of $M_{\alpha\beta}$ from the mean to be of the same order as the mean absolute value. This seems to be roughly true for both components of $m = 1$ but grossly untrue for the $i = 1$ component of $m = 2$. Since it is these mesoscopic fluctuations in $M_{\alpha\alpha}$ which determine the size of the ripples at the bottom of the Mexican Hat in the RMT scenario, this broad distribution of $M_{\alpha\beta}$ seems to be the cause of the failure of the RMT prediction that the ripples should be subdominant by $1/g$. While it is tempting to try to explain this in relation to the shape of the billiard (Fig. 2), which certainly appears to favor an $x^2 - y^2$ type of symmetry, a satisfactory explanation of the broad distribution of the $m = 2$, $i = 1$ matrix elements eludes us.

Our knowledge of the eigenfunctions at the global minimum allow us to compute the effective action for time-dependent σ at that minimum. Since the quasiparticles couple to this collective field, the interaction induces a decay width for the quasiparticles (details can be found in ref.[7]). In Fig. 11 we compare the numerically calculated values of the width to the parameter-free theoretical prediction (solid line) based on RMT[7]. On average, the RMT based prediction seems consistent with the numerics, though there is a lot of variation in the widths driven by large variations in the matrix elements coupling the quasiparticle levels to the collective mode.

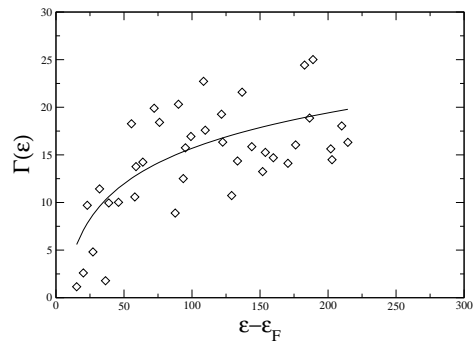


FIG. 11: A plot of the decay width of quasiparticles induced by their coupling to fluctuations of the collective field σ , for $N = 245$, $m = 2$, and $u = 2.15$. The solid line is the theoretical prediction from our previous RMT-based analysis[7]. While the prediction does well on average there are huge variations in the widths due to large variations in how strongly each level couples to the collective mode.

III. CONCLUSIONS

In our earlier work, we used a global RG assumption to reduce the problem on the scale of the Thouless energy to that of a disordered noninteracting problem with Fermi-liquid interactions. This is quite plausible for ballistic dots on very general grounds. To proceed further we had to make two further assumptions; (i) That the g approximate momentum states at the Fermi energy were a good basis in which to expand the exact disorder eigenstates, and (ii) That the wave functions of the exact eigenstates in the momentum basis obeyed all the statistical properties of RMT. Based on these two assumptions we were able to construct a solution to the problem which was asymptotically exact in the limit $g \rightarrow \infty$. This solution led to specific predictions for various physical quantities, including the size of the order parameter, the reduction in energy due to interactions, the shape of the energy landscape, and the size of the quasiparticle decay widths.

In this paper we have carried out a calculation which is still predicated on the validity of the Fermi-liquid form of the interactions on a scale E_L much larger than the Thouless energy E_T . In retaining this assumption we are on firm ground, since after all, the Thouless energy can be made as small as one wishes merely by increasing the size of the system. We also assumed that the mean-field description of the Landau Fermi-liquid interactions is valid, which is justified by the fact that the minima in the effective potential landscape are indeed of order $g^2\delta$. However, we explicitly eschewed the other two assumptions that we made in previous work, with a view to independently testing their validity. We found that our first assumption, that the approximate momentum states were a good basis in which to expand the exact disorder eigenstates, was extremely good near the Fermi energy, but became increasingly inaccurate as one went to the edge of the Thouless shell. We did not test the sec-

ond assumption about wavefunction correlations explicitly, but indirectly through its effects on the predictions of our earlier work. We found that most of the predictions held up, with the exception of the shape of the effective potential landscape in the case of symmetry-breaking in the $m = 2$ channel. Even here, the minimum is shaped more like a crescent, indicating the possible emergence of the Mexican Hat structure at larger values of g (we went to the largest value of g that we could given that we kept only 585 states and had to keep at least half the states empty). We traced the discrepancy back to the anomalously broad distribution (compared to estimates based on a complex gaussian distribution) of the matrix elements $M_{\alpha\beta}^x$. However, we were unable to pin down a physical reason for this broad distribution for the $m = 2$ case.

In conclusion, much of the physics we uncovered using our RMT assumptions seems to be valid in the Robnik-Berry billiard. The second-order transition that we uncovered in the $g \rightarrow \infty$ limit seems to indeed be broadened into a smooth crossover as expected, belying fears that it may be overtaken by a first-order bulk transition. The question of how large g has to be before RMT becomes

fully applicable remains open; another way to phrase the question is to ask what the nonuniversal corrections to RMT are in ballistic systems. Finally, an important open question is whether the broad distributions of matrix elements of interaction operators is a generic feature of ballistic systems, rather than being a special feature of the Robnik-Berry billiard, and if so, what physics determines the width of those distributions. However, our results here give us encouragement that the RMT assumptions can indeed be used with confidence in making predictions in ballistic systems, at a qualitative and semi-quantitative level.

IV. ACKNOWLEDGEMENTS

We would like to thank Yoram Alhassid, Alex Barnett, Piet Brouwer, and Doug Stone for illuminating conversations, and the Aspen Center for Physics where part of this work was carried out. We are also grateful to the NSF for partial support under grants DMR 0311761 (GM), DMR 0354517(RS).

-
- [1] U. Sivan *et al*, Phys. Rev. Lett. **77**, 1123 (1996); S. R. Patel *et al*, Phys. Rev. Lett. **80**, 4522 (1998); F. Simmel *et al*, Phys. Rev. B **59**, 10441 (1999); D. Abusch-Magder *et al*, Physica E **6**, 382 (2000); F. Simmel, T. Heinzl, and D. A. Wharam, Eur. Lett. **38**, 123 (1997); J. A. Folk *et al*, Phys. Rev. Lett. **86**, 2102 (2001); S. Lüscher *et al*, Phys. Rev. Lett. **86**, 2118 (2001).
 - [2] For recent reviews, see, T. Guhr, A. Müller-Groeling, and H. A. Weidenmüller, Phys. Rep. **299**, 189 (1998); Y. Alhassid, Rev. Mod. Phys. **72**, 895 (2000); A. D. Mirlin, Phys. Rep. **326**, 259 (2000).
 - [3] A. V. Andreev and A. Kamenev, Phys. Rev. Lett. **81**, 3199 (1998); P. W. Brouwer, Y. Oreg, and B. I. Halperin, Phys. Rev. B **60**, R13977 (1999); H. U. Baranger, D. Ullmo, and L. I. Glazman, Phys. Rev. B **61**, R2425 (2000); I. L. Kurland, I. L. Aleiner, and B. L. Al'tshuler, Phys. Rev. B **62**, 14886 (2000).
 - [4] I. L. Aleiner, P. W. Brouwer, and L. I. Glazman, Phys. Rep. **358**, 309 (2002), and references therein; Y. Oreg, P. W. Brouwer, X. Waintal, and B. I. Halperin, cond-mat/0109541, and references therein.
 - [5] G. Murthy and H. Mathur, Phys. Rev. Lett. **89**, 126804 (2002).
 - [6] G. Murthy and R. Shankar, Phys. Rev. Lett. **90**, 066801 (2003).
 - [7] G. Murthy, R. Shankar, D. Herman, and H. Mathur, Phys. Rev. B **69**, 075321 (2004).
 - [8] R. Shankar, *Physica* **A177**, 530 (1991); R. Shankar, Rev. Mod. Phys. **66**, 129 (1994).
 - [9] K. B. Efetov, Adv. Phys. **32**, 53 (1983); B. L. Al'tshuler and B. I. Shklovskii, Sov. Phys. JETP **64**, 127 (1986).
 - [10] M. L. Mehta, *Random Matrices*, Academic Press, San Diego, 1991.
 - [11] S. Chakravarty, B. I. Halperin, and D. R. Nelson, Phys. Rev. Lett. **60**, 1057 (1988); Phys. Rev. B **39**, 2344 (1989); For a detailed treatment of the generality of the phenomenon, see, S. Sachdev, *Quantum Phase Transitions*, Cambridge University Press, Cambridge 1999.
 - [12] M. Robnik, J. Phys. A **17**, 1049 (1984); M. V. Berry and M. Robnik, J. Phys. A **19**, 649 (1986).
 - [13] A. A. Abrikosov, L. P. Gorkov, and I. E. Dzyaloshinski, *Methods of Quantum Field Theory in Statistical Physics*, Dover Publications, New York, 1963.
 - [14] M. V. Berry, J. Phys. A **10**, 2083 (1977).
 - [15] A. D. Stone and H. Bruus, Physica B **189**, 43 (1993); Surface Science **305**, 490 (1994).
 - [16] Y. Alhassid and C. H. Lewenkopf, Phys. Rev. B **55**, 7749 (1997).
 - [17] K. B. Efetov and V. R. Kogan, Phys. Rev. B **67**, 245312 (2003), and references therein.
 - [18] S. Adam, P. W. Brouwer, and P. Sharma, Phys. Rev. B **68**, 241311 (2003)
 - [19] A. H. Barnett, private communication (2004).
 - [20] A. H. Barnett, "Asymptotic rate of quantum ergodicity in chaotic Euclidean billiards", Courant Institute preprint, 2004.